ELSEVIER

Bone Vol. 25, No. 6
December 1999:733–739

# Computer Simulation of Trabecular Remodeling Using a Simplified Structural Model

S. TAYYAR,[1] P. S. WEINHOLD,[2] R. A. BUTLER,[1] J. C. WOODARD,[3] L. D. ZARDIACKAS,[4] K. R. ST. JOHN,[4] J. M. BLEDSOE,[1] and J. A. GILBERT[1]

[1]*Department of Agricultural and Biological Engineering, Mississippi State University, Mississippi State, MS, USA*
[2]*Department of Orthopaedic Surgery, University of North Carolina, Chapel Hill, NC, USA*
[3]*Department of Comparative and Experimental Pathology, College of Veterinary Medicine, University of Florida, Gainesville, FL, USA*
[4]*Department of Biomaterials, University of Mississippi Medical Center, Jackson, MS, USA*

**A simplified three-dimensional simulation of trabecular bone remodeling has been developed. The model utilizes 441 planar structural units to represent approximately 50 mm$^3$ of initial bone volume with 199 basic multicellular units (BMUs). The simulation takes into account trabecular perforation in the structural model. The cases of male bone remodeling with no menopause and female bone remodeling with menopause are examined from the period of simulated age 25–80 years. Menopause is arbitrarily started at age 45 and extends for 7.5 years. Zero-, first-, and second-order BMU activation responses are employed to examine how the bone would be affected by the method of increase of BMU activation during menopause. At age 80, the female bone remodeling simulation produced a bone volume loss of approximately 49% for all three activation responses. This compared to a 38% bone volume loss for the case of no menopause. For the menopause simulations, an average of about 40% of the total bone loss was due to perforation. (Bone 25:733–739; 1999)** 

**Key Words:** Computer simulation; Trabecular remodeling; Bone loss; Perforation; Basic multicellular unit (BMU) activation rate.

## Introduction

Computer simulations of bone remodeling are attempts to correlate discrete physiological events with observed changes in bone morphology. Such computer simulations have been used by numerous researchers to investigate postmenopausal bone loss.[10–12,20,22] Although producing useful results, these previous simulations are essentially based on one-dimensional models, and therefore do not account for the interconnected trabecular structure of cancellous bone or the distribution of remodeling sites throughout that three-dimensional structure. However, the work of Thomsen et al.[21] stands out as a transition study that takes into account the importance of trabecular structural parameters in remodeling. The purpose of the current study is to utilize stochastic simulation of secondary trabecular bone remodeling to attempt to take into account the interconnected trabecular structure of cancellous bone and the associated remodeling site distribution.

Basic multicellular units (BMUs) are responsible for carrying out the bone remodeling process[5] and are also known as bone remodeling units or BRUs.[17] The BMU exists as the result of the antagonistic, coupled action of osteoclasts and osteoblasts that work together to replace old bone with new bone material. The life cycle of a BMU consists of four distinct phases: activation; resorption; reversal; and formation. The activation phase begins with an enabling act that proliferates osteoclastic precursors, which results in the appearance of osteoclasts.[9] Activation frequency, defined as the number of BMUs per unit volume of bone per unit time,[4] is generally considered one of the most important variables of remodeling. After activation, the resorption phase is carried out by the multinucleated osteoclasts that attach to the bone surface. The osteoclasts remove a packet of bone, leaving what is commonly known as a resorption cavity or Howship lacunae. The size of the resorption cavity depends on the number of osteoclasts present at the remodeling site during the resorption phase.[9] In the reversal phase, a cement line is laid down that separates the old bone not resorbed by the osteoclasts from the soon-to-be-deposited bone tissue. The formation phase is simply the formation of new bone carried out by osteoblasts that migrate to the resorption cavity. The osteoblasts lay down collagen and other bone matrix proteins that become mineralized to form new bone. The length of a BMU cycle is defined as the time elapsed between the beginning of the resorption and the end of the formation phases and is commonly termed the remodeling period, or sigma. The remodeling period value normally has a range of 3–6 months in humans, but can be as high as 1 year or more in patients with bone degenerative diseases such as osteoporosis.[6]

The end result of bone remodeling on a trabecula is a completed basic structural unit (BSU) at the remodeling site. A trabecular BSU has a semilunar structure (comprised of the packet of bone from the cement line to the marrow space) delineated by cement lines,[2] with the size of a single BSU varying from $50 \times 20$ to $1000 \times 1000$ $\mu m^2$ and averaging $200 \times 500$ $\mu m^2$ in size.[16] The net balance and volume of a BSU is determined by the activity level of the bone cells and the ratio of osteoblasts present during formation phase to the number of osteoclasts present during the resorption phase[9] and the relative activity of the bone cells. After the point of skeletal maturity,

*Address for correspondence and reprints:* Dr. Jerome A. Gilbert, Department of Agricultural and Biological Engineering, Box 9632, Mississippi State University, Mississippi State, MS 39762. E-mail: jgilbert@abe.msstate.edu





8756-3282/99/$20.00
PII S8756-3282(99)00218-5

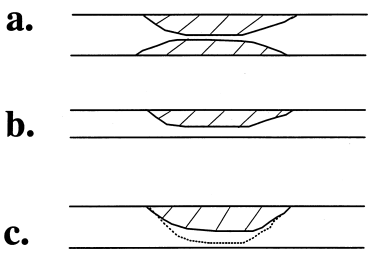


**Figure 1.** Three possible methods of trabecular perforation: (a) simultaneous remodeling on opposite sides of a trabecula; (b) resorption depth exceeding the thickness of a thin trabecula; and (c) the possible presence of excessively active osteoclasts that erode cavities that are deeper than normal.

there is a net decrease with age in trabecular bone volume seen in both men and women.[1,14] The decrease in trabecular bone volume has been attributed to a negative bone balance at the BMU level[2] and to trabecular perforation.

Compared to men, women experience excessive bone loss during the time period surrounding menopause.[3] Although the starting point and the length of menopause varies in women, the activation frequency of BMUs and the remodeling rate of both cortical and trabecular always increase due to a response to the decline in estrogen during menopause. The increased remodeling rate eventually returns to a rate parallel to that in men, but during the menopause period there is a net imbalance in resorption compared to formation and, consequently, a net bone loss. This net increased bone loss is thought to be a significant factor in the development of postmenopausal osteoporosis in women, because it correlates to an increased probability of trabecular perforation during menopause. Perforation is defined as the disconnection of trabeculae due to one of three hypothesized methods.[19,20] These methods are either simultaneous remodeling on both sides of the trabeculae (**Figure 1**a), resorption depth exceeding thin trabecular thickness (Figure 1b), or excessive resorption by "killer osteoclasts" that erode abnormally high amounts of bone tissue resulting in deeper than normal cavities (Figure 1c). The increased probability of trabecular perforation has been attributed to: (1) an increased probability of random coincidence of deep cavities and thin trabeculae as a result of increased activation rate and bone turnover due to reduction in estrogen levels; and (2) the possible presence of "killer osteoclasts" that erode deeper than normal cavities due to estrogen deficiency. Once perforation of a trabecula occurs, it is thought that the whole trabecular strut is then rapidly removed because of its non-load-bearing status.[16] This creates accelerated and irreversible bone loss.

It is now commonly known that a reduction in estrogen level increases BMU activation frequency.[8] In their computer simulations of bone remodeling, Kimmel[12] and Reeve[20] modeled the increase in BMU activation frequency due to decline in estrogen level as a zero-order response. However, Grodins[7] suggested that a change in activation stimulus to a control system is followed by a transient frequency response before steady state is achieved. According to Frost,[6] these transient responses will persist for one remodeling period before steady state is achieved by the system. Weinhold et al.[22] modeled the increase in BMU activation frequency responses to a step input decline in estrogen level as zero-, first-, and second-order transient BMU responses and produced significant findings concerning oscillatory BMU activation responses. The oscillatory responses may account for some of the transient bone remodeling events seen in women during menopause. Wienhold's simulation was, however, based on a one-dimensional model that failed to account for trabecular structure and remodeling site distribution and did not account for the occurrence of perforation.

The objective of this study was to expand the work of Weinhold et al.[22] by developing a simulation that is based on a two-/three-dimensional structural model of cancellous bone and that allows for the occurrence of trabecular perforation, a naturally occurring event. The cases of male (no menopause) and female (with menopause) bone remodeling are addressed. For the female case, the activation frequency response to the step decline

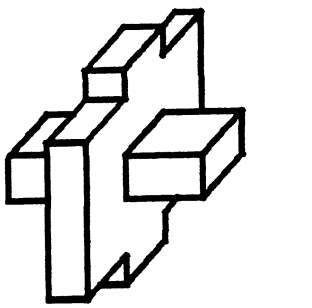

**Figure 2.** The basic structural unit for the simulation, based on the bar-plate trabecular structure.

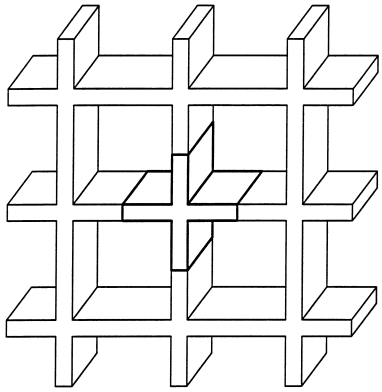

**Figure 3.** A planar representation of the three-dimensional bar-plate trabecular structure. The struts that extend out of the plane were replaced with an equivalent volume in the planar structure to simplify the analysis.

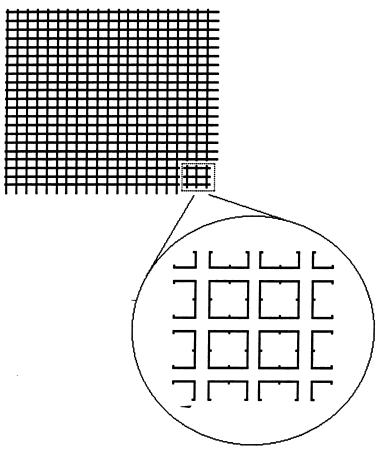

**Figure 4.** The total planar representation of the bone volume for the simulation. The inset shows the location of the center of the paired sites on opposite sides of each trabecula where remodeling could occur.

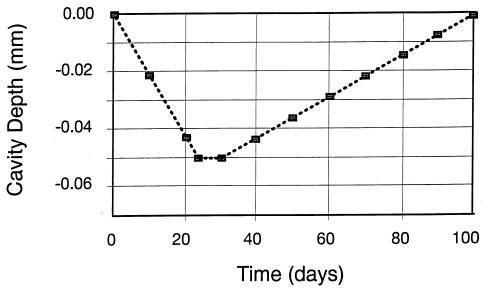


**Figure 5.** The depth of the resorption cavity as a function of remodeling days. There is a 2% underfilling of each remodeling site.

in estrogen level was modeled as a zero-, first-, and second-order response, in control theory terminology. The order of the response is the highest power of any of the derivatives in the equations dictating the feedback system response to a step input. It is speculated that a higher order response such as the second order or higher is occurring in the estrogen/activation-frequency control system. With more complex feedback systems, higher order systems are needed to describe the response.[22]

This study characterizes how bone loss, perforations, and the average trabecular width are altered for these cases. In contrast to previous studies, this simulation takes into account the interconnected structure of trabecular bone and the distribution of remodeling sites throughout that structure, thus giving a more complete picture of trabecular bone loss over time. In addition, the stochastic nature of this simulation conservatively models the spatial and temporal distribution of BMU formation.

## Materials and Methods

### *Model Parameters*

The simplified three-dimensional structural model in this simulation is based on a structure similar to the bar-plate trabecular structure.[15] The basic structural unit for this simulation is displayed in **Figure 2**. A total of 307 of these units are combined to create the trabecular bone model. For simplicity of programming, the volume of the bone struts in the third dimension was calculated, the struts removed in the third dimension, and an equivalent volume added as planar surface so that a planar representation of the three dimensions is created. This yields a total of 441

**Table 1.** Parameters used in computer simulation

| Parameter | Value |
|---|---|
| Number of BMUs | 199 |
| Tissue volume ($mm^3$) | 201.73584 |
| Bone volume ($mm^3$) | 49.63896 |
| Percent underfilling | 2% |
| Resorption cavity depth (mm) | 0.05 |
| Initial trabecular width (mm) | 0.14 |
| Trabecular thickness (mm) | 0.60 |
| Resorption period (days) | 24 |
| Reversal period (days) | 6 |
| Formation period (days) | 70 |
| Bone volume removed at the end of the resorption period ($mm^3$) | 0.018 |
| Bone volume formed at the end of the formation period ($mm^3$) | 0.01764 |
| Steady-state activation rate | 1 BMU/12 h |
| Menopause activation rate | 1 BMU/6 h |

BMU, basic multicellular unit.

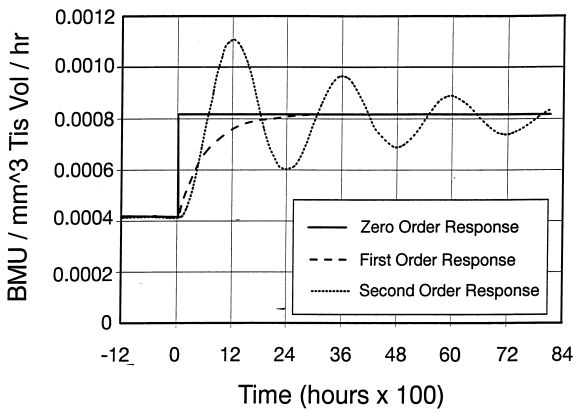


**Figure 6.** The three BMU activation responses to the abrupt step change in estrogen at menopause (where menopause time = 0 h).

planar structural units as is displayed in **Figure 3**. The model of Figure 3 is basically a two-dimensional model with a constant thickness in the third dimension.

The model shown in **Figure 4** has an initial bone volume of approximately 50 $mm^3$ (exact volume of 49.64 $mm^3$) with 199 BMUs.[4,22] This represents a bone volume of 24.8% of the tissue volume. Initially, all trabeculae possess the same width of 0.14 mm with a thickness in the third dimension of 0.60 mm. The total number of possible remodeling sites in the model is 1764, and the inset of Figure 4 shows the location of the sites with respect to the BMU. When a remodeling site is activated, a rectangular-shaped resorption cavity is created in the simulation to approximate the semilunar structure.

For simplicity, resorption and formation are assumed to be linearly dependent on time as seen in **Figure 5**. The resorption phase is represented as 24 days in length, with a maximum resorption cavity depth of 0.05 mm. The reversal phase that follows resorption lasts for 6 days. The subsequent formation phase is 70 days long. Formation results in a 2% underfilling of the resorption cavity. A list of the data used in the simulation is shown in **Table 1**.

The simulation was initialized for a small volume of bone from a theoretical person at the age of 25 years and run for the equivalent of 55 years, so that the ending age of the person was 80 years. The model was run for the case of no menopause to simulate the remodeling in a man and also for three cases of menopause response in women. A constant underfilling of the resorption cavity of 2% was used throughout for all cases. For the cases of menopause, zero-, first-, and second-order activation responses were run with the transient response of menopause beginning at age 45 and continuing through age 52.5 years. During the 7.5 year menopause phase, the activation frequency was taken to a level of double the premenopausal level. At age 52.5, the activation rate was returned to the premenopausal level.

An initial activation rate was based on 199 BMUs being active during any remodeling cycle (100 days). This gives an

**Table 2.** Average percent annual bone loss in simulation

| | Male bone (no menopause) | Menopause, zero order | Menopause, first order | Menopause, second order |
|---|---|---|---|---|
| Age 25–45 yr | 0.74[a] | 0.74[a] | 0.74[a] | 0.74[a] |
| Age 45–52.5 yr | 0.53 | 1.53 | 1.52 | 1.51 |
| Age 52.5–80 yr | 0.72 | 0.84 | 0.84 | 0.81 |

[a]0.53 without initial startup remodeling space.

Bone Vol. 25, No. 6
December 1999:733–739

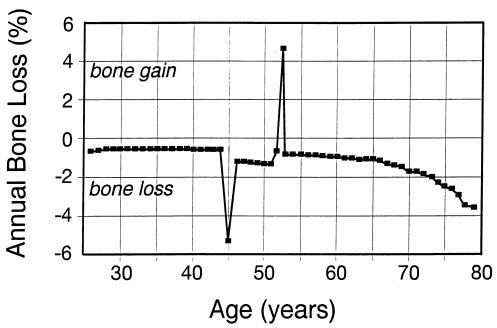


**Figure 7.** The annual trabecular bone loss for the zero-order menopause response. Menopause begins at age 45 years and ends at age 52.5 years in the computer simulation. The were no major differences between the zero-, first-, and second-order responses. A positive number represents a loss and a negative number represents a gain in bone volume.

initial activation rate of one BMU per 12 h. The zero-, first-, and second-order activation frequency responses to a step input decline in estrogen are shown in **Figure 6**. The equations regulating these responses have been described by Weinhold et al.[22] The zero-order response of a control system is described by Equation 1:

$$Y = Y' \tag{1}$$

where:

$$Y' = Y_0 \qquad t < 0$$

$$Y' = Y_{ss} \qquad t > 0$$

Equation 2 describes the first-order response of a control system:

$$Y = (Y_0 - Y_{ss})e^{-t/T} + Y_{ss} \tag{2}$$

where $T$ is the time constant of the control system that controls the response time of the system. The time constant was set to 560 h to achieve a response time of one remodeling period (100 days).

The second-order response of the control system is described by Equation 3:

$$Y = (Y_0 - Y_{ss})e^{-W_n tD}\{\cos(wt) + (D/[1 - D^2]^{1/2})\sin(wt)\} + Y_{ss} \tag{3}$$

where $D$ is the damping coefficient, which was set to 0.1 to describe an underdamped condition with oscillation. $W_n$ is the natural frequency, which controls the response time of the system. The natural frequency $W_n$ was set equal to 0.00263 $h^{-1}$, and it is defined by Equation 4:

$$W_n = (1/2400)2\pi \tag{4}$$

In each equation where present, $Y$ represents the activation frequency, $Y_0$ represents the initial activation frequency prior to the beginning of the transient response, and $Y_{ss}$ is the steady-state activation frequency that is approached by the transient response. For this simulation, $Y_0$ is set to 1 BMU per 12 h, and $Y_{ss}$ is 1 BMU per 6 h. In other words, during premenopause and postmenopause, the steady-state activation rate is 1 BMU per 12 h and perimenopausal rate is 1 BMU per 6 h.

### *Computer Analysis*

The code for this simulation was written in FORTRAN and consisted of a main program and 13 subroutines. At the beginning of the program, a 1764 × 100 array is declared, where the first dimension of the array represents the number of possible remodeling sites and the second dimension of the array is the number of elements in the array. The program array elements correspond to the following:

Element 1: initial trabecular width measured from the center line to the bone surface.
Element 2: record of the time a site has been active in a BMU.
Element 3: record of whether a site is active or inactive (1 = active, 0 = inactive).
Element 4: record of whether a site has perforated or not (1 = site has perforated, 0 = site has not perforated).
Element 5: updated cavity depth.
Element 6: bone volume removed due to remodeling.
Element >6: activation times for each BMU site.

A random number generator was used to determine which remodeling site was to be activated when an activation was to take place. The time step for the program was changed as needed to match the activation rate of the BMUs. For example, if the activation rate was one BMU per 12 h, then the time step was 12 h. If the activation rate was one BMU per 6 h, then the time step was 6 h. Prior to the running of the simulation, the activation response function was examined to determine the time step. For the second-order response, the time step changed constantly until steady state was achieved. Once a site was activated, it modeled the complete BMU cycle curve (Figure 5), with the trabecular width updated accordingly for every time step. Similarly, the bone volume removed due to remodeling was updated at every time step by multiplying the value of element 1 (updated trabecular width) by the size of the remodeling site (in $mm^2$). The removed bone volume was stored in element 6 of the array.

Perforation is defined to occur when the trabecular width between two opposite sites is <0.0.[20] Opposite sites on a trabecula are checked for perforation at every time step. When perforation occurs, the bone volume pertaining to these sites is added to the bone volume removed due to perforation and the numbers of sites lost due to perforation are advanced by two. The average trabecular width is also calculated every time step, which allows the user to check the status of the trabecular structure at any time.

Based on a 55 year simulation (age 25–80), four cases were

**Table 3.** Trabecular parameters at age 80 years in the simulation

| | Male bone (no menopause) | Menopause, zero order | Menopause, first order | Menopause, second order |
|---|---|---|---|---|
| Percentage of initial trabeculae that perforated | 8.11 | 21.94 | 21.71 | 20.58 |
| Average width | 0.08793 mm | 0.08055 mm | 0.08071 mm | 0.08103 mm |

examined: constant activation rate of one BMU per 12 h (male response) and three activation frequency responses. The main parameters recorded in the simulation were total bone volume lost, bone volume lost to perforation, bone volume lost to underfilling, number of perforating sites, location of perforated trabeculae, and average trabecular width. A display of the bone matrix was generated at the end of the simulation to display visually the location of the perforated trabeculae. Each of the four cases was run ten times, each with a different initial seed value for the random number generator that determined location of the activated BMU sites. The average of the ten runs was tabulated.

To document the effect of parameter changes on the model output, a limited sensitivity analysis was performed for the case of menopause with a zero-order activation response. The following standard model input parameters, as listed in Table 1, were varied: percent underfilling; resorption cavity depth; and the number of days apportioned to the three phases in the remodeling cycle. In the sensitivity analysis, underfilling was reduced to 1.5% and 1%, as compared to the standard of 2%. Resorption cavity depth was increased to 0.0525 mm and reduced to 0.0475 mm, as compared to the standard of 0.05 mm. Resorption, reversal, and formation days were changed to 30 + 6 + 64 and to 20 + 6 + 74, as compared to the standard of 24 + 6 + 70. A single run of the standard model was compared to single runs of the model with each parameter changed individually.

## Results

The average percentage of annual bone loss prior to menopause (age 25–45) was 0.74% for all four cases: constant activation rate (no menopause for the case of the male) and zero-, first-, and second-order responses. This included the initial volume of bone loss due to the remodeling space. The rate of loss with the remodeling space excluded was 0.53% of total bone volume per year. For the male bone simulation, the annual rate of loss increased to 0.72% in the 52.5–80 year period (postmenopause for the female bone simulations) due to the increased loss of bone as perforations occurred. For the three simulations with menopause, the rate of annual bone loss increased to 1.53%, 1.52%, and 1.51% for the zero-, first-, and second-order responses, respectively, during menopause (age 45–52.5). The average postmenopausal annual bone loss (age 52.5–80) was found to be 0.84%, 0.84%, and 0.81% for the zero-, first-, and second-order responses, respectively. **Table 2** shows a comparison of the responses.

The average annual bone loss as a percentage of bone volume for the zero-order response is shown in **Figure 7**. A sharp increase can be seen at age 46 corresponding to the increase in remodeling space that was a direct result of the increase in activation rate. A sharp decrease is seen at age 53, which was due to the decrease in the activation frequency and a corresponding decrease in remodeling space. The nonlinear trend beyond age 65 was due to the increasing amount of bone loss due to perforation. The lowest average trabecular width of 0.08055 mm was reached with the zero-order response, and the highest average width of 0.08793 mm was obtained for the male bone case that had a constant activation rate. A list of trabecular width of all cases is shown in **Table 3**. **Figure 8** plots the trabecular width as it relates to age for the zero-order response. About 40% of the trabecular width was lost due to thinning over the course of the simulation.

**Table 4.** Percent cumulative bone loss at age 80 years in the simulation

| | Male bone (no menopause) | Menopause, zero order | Menopause, first order | Menopause, second order |
|---|---|---|---|---|
| Due to perforation | 7.28 | 19.67 | 19.45 | 18.46 |
| Due to negative balance | 30.58 | 29.67 | 29.69 | 29.94 |
| Total loss | 37.87 | 49.34 | 49.14 | 48.40 |

The average total bone volume lost at age 80 was 18.80 $mm^3$ for the constant activation rate (no menopause), and it was 24.49 $mm^3$, 24.39 $mm^3$, and 24.03 $mm^3$ for the zero-, first-, and second-order rates, respectively. This corresponds to percentage losses of 37.87%, 49.34%, 49.14%, and 48.40%, respectively (**Table 4**). These results demonstrate no significant differences in terms of bone loss among the three transient responses. The cumulative bone loss for the total simulation for the zero order response is shown in **Figure 9**. Comparing the values for the zero-, first-, and second-order responses to the average total loss of 18.80 $mm^3$ (37.87%) in the case of the male bone simulation, one can see that the additional loss due to the increase in activation rate associated with menopause ranged from 10.54% to 11.5%. This increase in activation rate resulted in a transient increase in the remodeling space, because there were twice as many BMUs active in the cancellous network during the simulated menopause.

The percentage of the original bone volume lost due to perforation was 19.67%, 19.45%, and 18.46% for the zero-, first-, and second-order responses, respectively (Table 4). When the lost bone volume was divided between perforation and underfilling, it became apparent that trabecular perforation was a significant contributor to the loss for the menopause cases. The ratio of perforated loss to total bone loss was 0.399, 0.396, and 0.381 for the zero-, first-, and second-order responses. The ratio of perforation loss to total loss for the no menopause, male bone

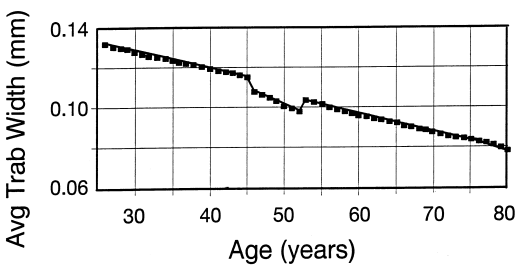


**Figure 8.** Average trabecular width as a function of age in the zero-order menopause response.

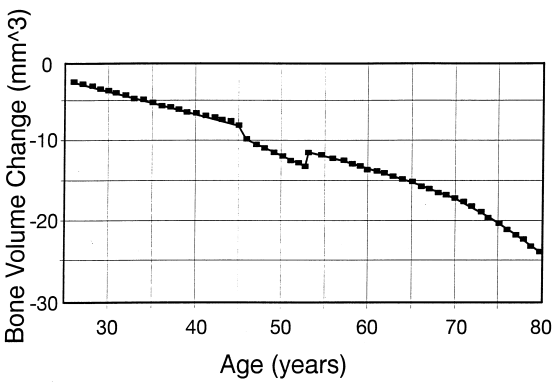


**Figure 9.** Cumulative trabecular bone volume change for the zero-order menopause response.

Bone Vol. 25, No. 6
December 1999:733–739

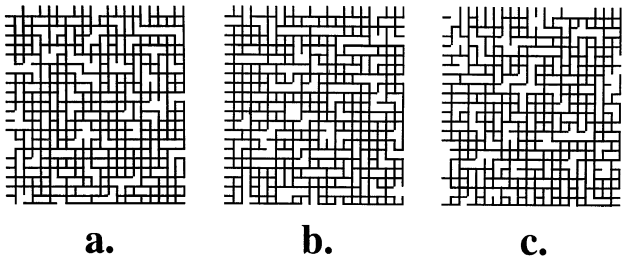


**Figure 10.** Trabecular matrix at age 80 years for three different runs of the zero-order menopause response. The three displays represent a minimum (a), an average (b), and the maximum (c) amount of bone loss due to perforation. The percentage of the initial trabeculae that perforated are 20.4%, 21.5%, and 23.5%, respectively.

simulation was 0.192. The first perforation for the case of the male bone simulation occurred at age 60. This compares to age 54, 54, and 55 years for the zero-, first-, and second-order responses, respectively. The total number of perforating sites at age 80 were 143, 387, 383, and 363 for the constant, zero-, first-, and second-order responses, respectively, and constitutes 8.11%, 21.94%, 21.71%, and 20.58% of the total remodeling sites (Table 3).

The trabecular structure at age 80 is shown in **Figure 10**a–c for three different seed values, out of ten, using the zero-order response. They represent the minimum, average, and maximum number of perforations obtained with the different seed values. The percentages of trabeculae lost due to perforations are 20.41%, 21.54%, and 23.47%, respectively, for these cases.

The results of the sensitivity analysis are presented in **Table 5** for a single run of the simulation with each of the following parameters varied individually: underfilling percentage of the resorption cavity; resorption cavity depth; and relative values of the days for resorption, reversal, and formation. Decreasing the underfilling decreased the total bone lost and greatly decreased the perforation percentage. Increasing and decreasing the depth of the resorption cavity had the similar effect of increasing and decreasing bone lost and perforations. The changing of the number of days of resorption and formation did not have a great effect on bone loss or perforations.

## Discussion

For trabecular bone, the calculated annual average bone loss in the case of constant activation rate of one BMU per 12 h is 0.53% (without the remodeling space) or 0.74% with the remodeling space. This is in agreement with the reported annual trabecular bone loss of 5% per decade in men up to age 90 years.[13] The postmenopausal average trabecular annual bone loss of 0.84% is lower, however, than the annual postmenopausal bone loss of 1.39% reported by Parfitt.[17] The difference in annual postmenopausal bone loss can be attributed to the limitation of the current parameter values in the model. For the model to match exactly the observed responses in vivo, the model will need further structural refinement so that it possesses a structure more like actual bone. It should be noted that this model is focused only on trabecular bone, which makes up only about 20% of the total skeletal mass.

This model does take a major first step in adding the concept of structural form to the study of bone simulation. The matrix construct allows underfilling and perforation to simultaneously impact bone volume in a spatial manner. Perforation was shown to be a significant factor in the overall bone loss, about 40% of the total bone loss. The impact of perforation on overall bone loss that was apparent in this model is an interesting finding and a close examination of the trabecular structure at age 80 years shows perforations to be uniformly distributed over the entire structure. This was not surprising because the location of new remodeling sites was a purposefully random process in the simulation. No major differences were seen between the three activation responses for any of the parameters monitored. The idealized response to a step input is the zero-order, instantaneous response. Excluding the idealized zero-order system, it can be generalized that higher order control systems (orders $>1$) exhibit quicker responses to input signals and may tend to exhibit some overshoot in the attempt to quickly reach an equilibrium response level. The quick response and the overshoot should tend to simulate increased synchronization of the resorption cycles in remodeling. It is speculated that the lack of difference between the lower and higher ordered response systems in the current study may be due to the simplistic nature of this first-step model. As a model of trabecular bone takes on more of the structural and physiological complexity of actual bone, the activation response models may display significantly different results.

The bone simulation model in this project was intentionally created to mimic the actual structure and cellular remodeling events that occur in secondary trabecular bone. To have the model actually behave in a fashion similar to that observed in human trabecular bone, all of the simulation parameters were set to values within the range observed for actual trabecular bone. The parameters were adjusted within the observed range to have the chief output parameter, bone volume lost, match accepted human levels. Because human trabecular bone would be very sensitive to changes in parameters, such as average resorption depth and the percent underfilling of resorption cavities during formation, it was anticipated that the simulation model would likewise be sensitive to changes in these parameters. The sensi-

**Table 5.** Sensitivity analysis performed for the case of menopause with a zero-order response

| | Percent bone loss at age 80 yr | Percentage of initial trabeculae that perforated at age 80 yr |
|---|---|---|
| Original model: 2% underfilling; resorption cavity depth of 0.05 mm; remodeling days: 24 resorption, 6 reversal, 70 formation | 49.44 | 22.11 |
| Resorption cavity with 1% underfilling | 20.77 | 0.00 |
| Resorption cavity with 1.5% underfilling | 30.34 | 2.15 |
| Resorption cavity depth of 0.0525 mm | 66.88 | 50.68 |
| Resorption cavity depth of 0.0475 mm | 39.12 | 6.92 |
| Remodeling days changed to: 30 resorption, 6 reversal, 64 formation | 48.37 | 20.29 |
| Remodeling days changed to: 20 resorption, 6 reversal, 74 formation | 50.18 | 23.47 |

tivity analysis proved these speculations to be true. As expected, underfilling percentage had a large effect on bone volume lost and the corresponding perforations. Resorption cavity depth also had a significant impact. The change in resorption, reversal, and formation days had only a slight impact on the output parameters.

The results of the current model would obviously have been affected by including a distribution of trabecular widths and erosion depths. Because the model was an initial first step at incorporating three-dimensional morphology into a bone loss simulation, the number of complicating variables was held to a minimum so as to demonstrate clearly an actual bone loss response. A logical refinement of the model would be to include a distribution of parameters, as was done by Thomsen et al.[21] The current study differs from Thomsen et al.[21] in that it included a spatial distribution and interconnection of the modeled trabecular struts in the simulation, whereas Thomsen et al. did not attempt to assign each trabecula a unique position in space.

Further refinement of the model could include more complex trabecular interconnections. It would also be logical to allow for the physical overlapping of potential bone remodeling sites. The current model requires that the remodeling sites be situated end to end with no potential overlap of the remodeling areas. This overlapping concept could be extended to include overlapping time steps also, so that one BMU could be superimposed on another. Thus, the "piggyback" effect seen in natural bone remodeling may also be accounted for. The reversal and formation periods could also be adjusted, which would impact the occurrence of perforation.

Additional improvements to the model could include using finite-element analysis to influence the locating of new remodeling sites based on mechanical stresses at the sites. By doing so, one may achieve results in which the trabeculae are preferentially activated and/or perforated in a given direction or plane. It may therefore be possible to use this model to simulate trabecular bone loss under preformulated load conditions that are tied to stresses seen in normal function. Then remodeling sites would no longer be generated or distributed on a random basis, but would have mechanical stress as a modulating variable. Other variables could also be investigated to better simulate the three-dimensional evolution of the BMU.[18]

Further simulations, refinements, and initial conditions may prove useful in leading to a more complete understanding of the trabecular bone remodeling phenomenon. In any case, a model with structural form, such as the one in this study, will be useful in moving toward a more realistic remodeling simulation where the locations of remodeling sites and perforations are of critical importance.

*Acknowledgments:* This work was supported by NIH Grant 1R15AR41540-01 and Mississippi Agricultural and Forestry Experiment Station Grant MIS-6809. This study was approved for publication as Journal Article No. J-9165 of the Mississippi Agricultural and Forestry Experiment Station, Mississippi State University. The authors are grateful to Dr. Lung-Hua Chen for his assistance in the review of the manuscript. This research was performed in partial fulfillment of requirements for a doctoral degree from Mississippi State University by Saleh Tayyar.

## References

1. Courpron, P. Bone tissue mechanisms underlying osteoporoses. Orthop Clin N Am 12:513–545; 1981.
2. Eriksen, E. F. Normal and pathological remodeling of human trabecular bone: Three dimensional reconstruction of the remodeling sequence in normals and in metabolic bone disease. Endocrin Rev 7:379–408; 1986.
3. Eriksen, E. F., Mosekilde, L., and Melsen, F. Trabecular bone resorption depth decreases with age: Differences between normal males and females. Bone 6:141–146; 1985.
4. Frost, H. M. Mathematical Elements of Lamellar Bone Remodeling. Springfield, IL: Thomas; 1964.
5. Frost, H. M. The Intermediate Organization of the Skeleton. Boca Raton, FL: CRC; 1986.
6. Frost, H. M. Bone histomorphometry: Analysis of trabecular bone dynamics. In: Recker, R. R., Ed. Bone Histomorphometry: Techniques and Interpretation. Boca Raton, FL: CRC; 1983; 109–131.
7. Grodins, F. S. Control Theory and Biological Systems. New York: Columbia University; 1963.
8. Heaney, R. P. A unified concept of osteoporosis. Am J Med 39:877–880; 1965.
9. Jaworski, Z. F. G. Histomorphometric characteristics of metabolic bone disease. In: Recker, R. R., Ed. Bone Histomorphometry: Techniques and Interpretation. Boca Raton, FL: CRC; 1983; 241–263.
10. Kimmel, D. B. A computer simulation of the adult bone remodeling system. In: Proceedings of the 1983 Summer Computer Simulation Conference, North Holland, Amsterdam; 1983, 744–749.
11. Kimmel, D. B. A computer simulation of the mature skeleton. Bone 6:369–372; 1985.
12. Kimmel, D. B. A discrete event simulation of the mature skeleton. Math Model 7:957–980; 1986.
13. Mazess, R. B. On aging bone loss. Clin Orthop Rel Res 165:239–252; 1982.
14. Melsen, F., Melsen, B., Mosekilde, L. E., and Bergmann, S. Histomorphometric analyses of normal bone from the iliac crest. Acta Pathol Microbiol Scand 86:70–81; 1978.
15. Morita, M., Ebihara, A., Itoman, M., and Sassada, T. Progression of osteoporosis in cancellous bone depending on trabecular structure. Ann Biomed Eng 22:532–539; 1994.
16. Mosekilde, L. Consequences of the remodeling process for the vertebral trabecular bone structure: A scanning electron microscopy study (uncoupling of unloaded structures). Bone Miner 10:13–35; 1990.
17. Parfitt, A. M. Quantum concept of bone remodeling and turnover: Implications for the pathogenesis of osteoporosis. Calcif Tissue Int 28:1–5; 1979.
18. Parfitt, A. M. Osteonal and hemi-osteonal remodeling: The spatial and temporal framework for signal traffic in adult human bone. J Cell Biochem 55:273–286; 1994.
19. Parfitt, A. M., Mathews, H. E., Villanueva, A. R., Kleerekoper, M., Frame, B., and Rao, D. S. Relationships between surface, volume, and thickness of iliac trabecular bone in aging and in osteoporosis. J Clin Invest 72:1396–1409; 1983.
20. Reeve, J. A stochastic analysis of iliac trabecular bone dynamics. Clin Orthop Rel Res 213:264–278; 1986.
21. Thomsen, J. S., Mosekilde, L., Boyce, R. W., and Mosekilde, E. Stochastic simulation of vertebral trabecular bone remodeling. Bone 15:655–666; 1994.
22. Weinhold, P. S., Gilbert, J. A., and Woodard, J. C. The significance of transient changes in trabecular bone remodeling activation. Bone 15:577–584; 1994.

*Date Received:* February 3, 1999
*Date Revised:* August 9, 1999
*Date Accepted:* August 13, 1999